Journal of Molecular Catalysis B: Enzymatic 63 (2010) 179–187

Contents lists available at ScienceDirect

Journal of Molecular Catalysis B: Enzymatic

journal homepage: www.elsevier.com/locate/molcatb

Oxidation of human cytochrome P450 1A2 substrates by *Bacillus megaterium* cytochrome P450 BM3

Dong-Hyun Kim[a], Keon-Hee Kim[a], Dooil Kim[b], Heung-Chae Jung[b], Jae-Gu Pan[b], Youn-Tai Chi[a], Taeho Ahn[c], Chul-Ho Yun[a,*]

[a] School of Biological Sciences and Technology, Chonnam National University, Buk-gu, Yong-bong 300, Gwangju 500-757, Republic of Korea
[b] Systems Microbiology Research Center, Korea Research Institute of Bioscience and Biotechnology, Daejeon 305-806, Republic of Korea
[c] College of Veterinary Medicine, Department of Biochemistry, Chonnam National University, Gwangju 500-757, Republic of Korea

ARTICLE INFO

Article history:
Received 14 September 2009
Received in revised form 20 January 2010
Accepted 20 January 2010
Available online 28 January 2010

Keywords:
Drug metabolism
Human drug metabolites
Human P450 1A2
Oxidation
P450 BM3

ABSTRACT

Cytochrome P450 enzymes (P450s or CYPs) are good candidates for biocatalysis in the production of fine chemicals, including pharmaceuticals. Despite the potential use of mammalian P450s in various fields of biotechnology, these enzymes are not suitable as biocatalysts due to their low stability, low catalytic activity, and limited availability. Recently, wild-type and mutant forms of bacterial P450 BM3 (CYP102A1) from *Bacillus megaterium* have been found to metabolize various. It has therefore been suggested that CYP102A1 may be used to generate the metabolites of drugs and drug candidates. In this report, we show that the oxidation reactions of typical human CYP1A2 substrates (phenacetin, ethoxyresorufin, and methoxyresorufin) are catalyzed by both wild-type and mutant forms of CYP102A1. In the case of phenacetin, CYP102A1 enzymes show only *O*-deethylation product, even though two major products are produced as a result of *O*-deethylation and 3-hydroxylation reactions by human CYP1A2. Formation of the metabolites was confirmed by HPLC analysis and LC–MS to compare the metabolites with the actual biological metabolites produced by human CYP1A2. The results demonstrate that CYP102A1 mutants can be used for cost-effective and scalable production of human CYP1A2 drug metabolites. Our computational findings suggest that a conformational change in the cavity size of the active sites of the mutants is dependent on activity change. The modeling results further suggest that the activity change results from the movement of several specific residues in the active sites of the mutants.

1. Introduction

Cytochrome P450 (P450 or CYP for a specific isoform) enzymes constitute a large family of enzymes that are remarkably diverse oxygenation catalysts found throughout all classes of life (http://drnelson.utmem.edu/CytochromeP450.html). This family of proteins is found in archaea, bacteria, fungi, plants, and animals. Due to their catalytic diversity and broad substrate range, P450s are attractive biocatalyst candidates for the production of pharmaceuticals and fine chemicals and for the optimization of lead compounds [1–3]. Despite the potential for mammalian P450s for use in various biotechnological applications, they are, in reality, unsuitable as biocatalysts due to low stability, low catalytic activity, and limited availability.

In contrast, the soluble CYP102A1 (P450 BM3) enzyme from *Bacillus megaterium* does appear to be a good biocatalyst candidate for use in the pharmaceutical industry [4]. In this enzyme, the soluble reductase domain is fused to the C-terminus of the catalytic heme domain in a single polypeptide. The fusion of these two enzymatic activities makes soluble CYP102A1 an ideal model for mammalian, and in particular human, P450 enzymes.

P450s are involved in the metabolism of most (>80%) drugs currently available on the market. If pro-drugs are found to be converted to biologically 'active metabolites' by the liver P450s during the drug development process, the metabolites are required to understand the drug's efficacy, toxic effects, and pharmacokinetics [5]. Recently, it was shown that various CYP102A1 mutants generated by random and site-directed mutagenesis can oxidize several human P450 substrates to produce authentic metabolites [3,4,6–14]. This suggests that the use of CYP102A1 engineered with the desired properties is a viable alternative approach for preparing metabolites from drugs and drug candidates.

Abbreviations: CYP or P450, cytochrome P450; CPR, NADPH-cytochrome P450 reductase; LC–MS, liquid chromatography–mass spectrometry; PhOD, phenacetin *O*-deethylation; EROD, 7-ethoxyresorufin *O*-deethylation; MROD, 7-methoxyresorufin *O*-deethylation; αNF, 7,8-benzoflavone.

* Corresponding author. Tel.: +82 62 530 2194; fax: +82 62 530 1919.
E-mail address: chyun@jnu.ac.kr (C.-H. Yun).

1381-1177/$ – see front matter © 2010 Elsevier B.V. All rights reserved.
doi:10.1016/j.molcatb.2010.01.017

Human CYP1A2, one of the major hepatic P450s in the liver (constituting 10–15% of the total P450 content of the human liver), metabolizes about 15% of clinical drugs and bioactivates a number of procarcinogens, carcinogenic aryl, and heterocyclic amines [15]. This enzyme plays a dominant role in the metabolic clearance of caffeine and melatonin, as well as the clearance of clinical drugs such as flutamide, lidocaine, olanzapine, tacrine, theophylline, triamterene, and zolmitriptan [16]. *O*-Deethylation reactions of phenacetin, 7-ethoxycoumarin, and 7-ethoxyresorufin are commonly used assays for determining CYP1A2 activity *in vitro* [17].

In this study, we examined the catalytic properties of the wild-type and mutant forms of CYP102A1 to oxidize typical (phenacetin) and test substrates (7-ethoxyresorufin, and 7-methoxyresorufin) of human CYP1A2 to generate human metabolites. Phenacetin is an analgesic, and therefore its oxidation by bacterial P450 provides new reference substances for the pharmaceutical industry [18]. 7-Ethoxyresorufin and 7-methoxyresorufin have already been used for screening of CYP102A1 mutants [4,14]. These alkoxyresorufin substrates were found to be useful for identifying high active mutants when they were used with other alkoxyresorufin substrates, benzyloxyresorufin and pentoxyresorufin [4]. A set of CYP102A1 mutants was used to determine whether these enzymes are capable of oxidizing typical substrates of human CYP1A2, and we found that the substrates were oxidized by a set of the CYP102A1 mutants. These results suggest that CYP102A1 mutants can be developed as "humanized" bacterial monooxygenases for biotechnological applications.

2. Materials and methods

2.1. Materials

Phenacetin, acetaminophen, and 7,8-benzoflavone (αNF) were purchased from Sigma–Aldrich (Milwaukee, WI). 7-Ethoxyresorufin, 7-methoxyresorufin, and 7-OH resorufin were obtained from Invitrogen (Carlsbad, CA). Other chemicals were of the highest grade commercially available.

2.2. Construction of CYP102A1 mutants by site-directed mutagenesis

Seventeen different site-directed mutants of CYP102A1 were prepared as described [7 and references therein]. Most of the CYP102A1 mutants used in this study were selected based on earlier work showing their increased catalytic activity toward several human substrates. Each mutant bears the following amino acid substitution(s) relative to wild-type CYP102A1: 1 (F87A) [19]; 2 (A264G) [19]; 3 (F87A/A264G) [19]; 4 (R47L/Y51F) [19]; 5 (R47L/Y51F/A264G) [19]; 6 (R47L/Y51F/F87A) [19]; 7 (R47L/Y51F/F87A/A264G) [19]; 8 (A74G/F87V/L188Q) [20]; 9 (R47L/L86I/L188Q) [7]; 10 (R47L/F87V/L188Q) [4]; 11 (R47L/F87V/L188Q/E267V) [4]; 12 (R47L/L86I/L188Q/E267V) [7]; 13 (R47L/L86I/F87V/L188Q) [4]; 14 (R47L/F87V/E143G/L188Q/E267V) [7]; 15 (R47L/E64G/F87V/E143G/L188Q/E267V) [7]; 16 (R47L/F81I/F87V/E143G/L188Q/E267V) [7]; 17 (R47L/E64G/F81I/F87V/E143G/L188Q/E267V) [4].

2.3. Expression and purification of CYP102A1 mutants

The plasmids of wild-type CYP102A1 (pCWBM3) and mutant CYP102A1 were transformed into *Escherichia coli* strain DH5αIQ (Invitrogen, Carlsbad, CA), according to the manufacturer's instructions. The first culture was inoculated from a single colony into 5 ml of Luria–Bertani medium supplemented with 100 μg/ml ampicillin and grown at 37 °C. This culture was used to inoculate 250 ml of Terrific Broth medium supplemented with 100 μg/ml ampicillin. The cells were grown at 37 °C, with shaking at 250 rpm, to an $OD_{600} \sim 0.8$, at which time gene expression was induced by addition of isopropyl-β-D-thiogalactopyranoside to a final concentration of 0.50 mM. δ-Aminolevulinic acid (1.0 mM) was also added. Following induction, the cultures were allowed to grow for another 36 h at 30 °C. Cells were harvested by centrifugation (15 min, 5000 × *g*, 4 °C). The cell pellet was resuspended in TES buffer [100 mM Tris–HCl (pH 7.6), 500 mM sucrose, 0.5 mM EDTA] and lysed by sonication (Sonicator, Heat Systems—Ultrasonic, Inc.). After the lysate was centrifuged at 100,000 × *g* (90 min, 4 °C), the soluble cytosolic fraction was collected and used for the activity assay. The cytosolic fraction was dialyzed against 50 mM potassium phosphate buffer (pH 7.4) and stored at −80 °C. Enzymes were used within 1 month of purification. CYP102A1 concentrations were determined from the CO-difference spectra, as described by Omura and Sato [21], using $\varepsilon = 91\ mM^{-1}\ cm^{-1}$. For all of the wild-type and mutated enzymes, a typical culture yielded 300–700 nM of P450 protein. The expression level of wild-type and mutant CYP102A1 was in the range of 1.0–2.0 nmol P450 per mg of cytosolic protein.

2.4. Enzyme assays

Several typical substrates of human CYP1A2 have been used to examine the catalytic activities of wild-type and mutant forms of CYP102A1, as described below (Fig. 1). Typical steady-state reactions for phenacetin *O*-deethylation (PhOD), 7-methoxyresorufin *O*-deethylation (MROD), and 7-ethoxyresorufin *O*-deethylation (EROD), were composed of 50 pmol of CYP102A1 in 0.50 ml of 100 mM potassium phosphate buffer (pH 7.4) along with a specified amount of substrate for 10 min. To determine the turnover numbers of wild-type CYP102A1 and all tested mutants, we used substrates at concentrations of 2.0 μM, 2.0 μM, and 2.0 mM for 7-methoxyresofufin, 7-ethoxyresorufin, and phenacetin, respectively. In human CYP1A2 activity assays, a control experiment of 50 pmol P450, 100 pmol NADPH-P450 reductase (CPR), and 45 μM L-α-dilauroyl-*sn*-glycero-3-phosphocholine (DLPC) was used instead of 50 pmol CYP102A1.

EROD and MROD: MROD and EROD activities were measured using a fluorescence assay [22]. The reaction mixtures contained 50 pmol CYP102A1 enzyme, 100 mM potassium phosphate buffer (pH 7.4), an NADPH-generating system (0.5 mM $NADP^+$, 10 mM glucose 6-phosphate, and 1.0 IU glucose 6-phosphate dehydrogenase ml^{-1}), and varying concentrations of substrate (0.1–20 μM) in a total volume of 0.5 ml. Pre-incubations with the reaction mixture were generally carried out for 10 min at 37 °C. The reaction was initiated by the addition of the NADPH-generating system, incubated for 10 min at 37 °C, and terminated with 1.0 ml of CH_3OH. Metabolites were measured using fluorescence and a resorufin standard [23].

Phenacetin O-deethylation (*PhOD*): The reaction mixtures consisted of 50 pmol CYP102A1, 100 mM potassium phosphate buffer (pH 7.4), an NADPH-generating system, and varying concentrations of substrate (0.01–2.0 mM phenacetin) in a total volume of 0.25 ml. PhOD activity was determined by HPLC as described [18]. Briefly, incubations with the reaction mixture were performed for 20 min at 37 °C, terminated with 0.5 ml of 17% $HClO_4$, and centrifuged ($10^3 \times g$, 10 min); 0.5 ml of a mixture of $CHCl_3$ and 2-propanol (6:4, v/v) was added to the supernatant to extract the products, followed by centrifugation (twice at $10^3 \times g$ for 30 min). The organic layers were combined, and the solvent was removed under N_2 gas. The products (acetaminophen and the acetol) were analyzed by HPLC using a Gemini C_{18} column (4.6 mm × 150 mm, 5 μm, Phenomenex)

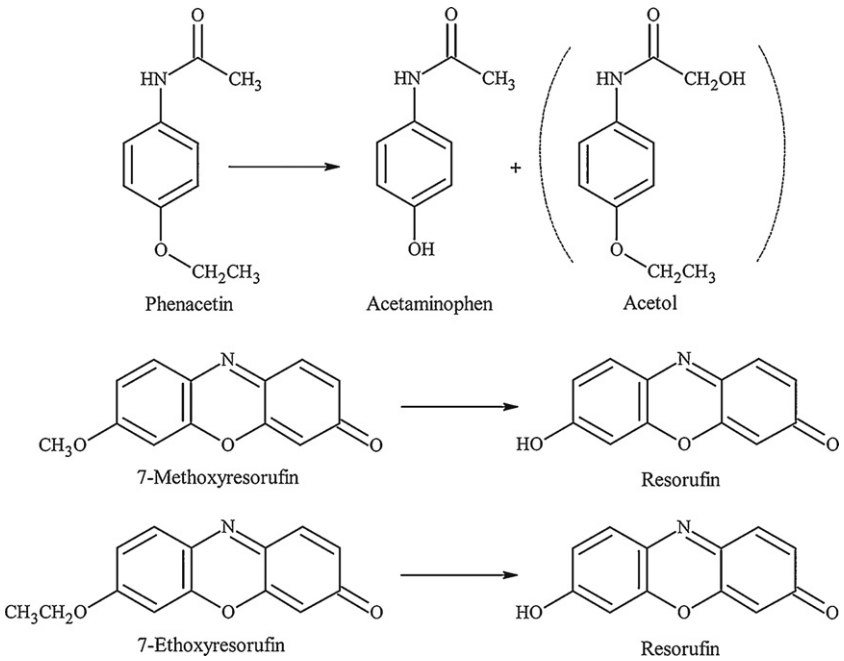

Fig. 1. Chemical structures of phenacetin, 7-ethoxyresorufin, 7-methoxyresorufin, and their metabolites. The conversion of substrates to their corresponding products is catalyzed by P450 enzymes in the presence of NADPH. The acetol product of phenacetin is formed only by human CYP1A2, not by CYP102A1.

with a mobile phase of $H_2O/CH_3OH/CH_3CO_2H$ (65:35:0.1, v/v/v; flow rate 1.0 ml min^{-1}), monitoring at A_{254}.

Kinetic parameters (K_m and k_{cat}) were determined using nonlinear regression analysis with GraphPad PRISM software (GraphPad, San Diego, CA, USA). The data were fit to the standard Michaelis–Menten equation: $v = k_{cat}[E][S]/([S] + K_m)$. In this equation, the velocity of the reaction is a function of the rate-limiting step in turnover (k_{cat}), the enzyme concentration ([E]), substrate concentration ([S]), and the Michaelis constant (K_m).

2.5. Liquid chromatography-mass spectrometry (LC–MS) analysis of phenacetin and its metabolites

The reaction residue was reconstituted into 100 μl of mobile phase by vortex mixing and sonication for 20 s. An aliquot (5 μl) of this solution was injected onto the LC column. LC–MS analysis was carried out on a Shimadzu LCMS-2010 EV system (Shimadzu Corporation, Japan) with the LC–MS solution software in electro spray ionization (positive) mode. The separation was performed on a Shim-pack VP-ODS column (2.0 mm i.d. × 250 mm, Shimadzu Corporation, Japan) using a mobile phase of methanol and water (35:65, v/v) containing 2.5 mM formic acid at a flow rate of 0.18 ml/min. To identify the metabolites, mass spectra were recorded by electro spray ionization in positive mode. Interface and detector voltages were set at 4.4 and 1.5 kV, respectively. Nebulization gas flow was set at 1.5 l/min. Interface, curve desolvation line (CDL), and heat block temperatures were 250, 230, and 200 °C, respectively.

2.6. Total turnover numbers (TTNs)

Reaction mixtures contained 50 pmol P450, 100 mM potassium phosphate buffer (pH 7.4), an NADPH-generating system, and substrate (2.0 mM and 20 μM of phenacetin and 7-ethoxyresorufin, respectively). The reaction mixtures were incubated at 30 °C for 6 h, and the products of phenacetin and 7-ethoxyresorufin were analyzed by HPLC and with a fluorometer, respectively, as described above.

2.7. Effects of 7,8-benzoflavone (αNF) on the O-deethylation reactions catalyzed by CYP102A1 enzymes

Reaction mixtures contained 50 pmol P450, 100 mM potassium phosphate buffer (pH 7.4), an NADPH-generating system, substrate (2.0 mM and 20 μM of phenacetin and 7-ethoxyresorufin, respectively), and 200 μM 7,8-benzoflavone (αNF). Products were analyzed by HPLC and with a fluorometer, respectively, as described above.

2.8. Spectral binding titrations

Spectral binding titrations were used to determine dissociation constants (K_s) for substrates and products, as previously described [24]. Binding affinities of ligands to CYP102A1 enzymes were determined (at 23 °C) by titrating 1.5 μM enzyme with the ligand, in a total volume of 1.0 ml of 100 mM potassium phosphate buffer (pH 7.4). Final CH_3CN concentrations were <2% (v/v). Spectral dissociation constants (K_s) were estimated using GraphPad Prism software (GraphPad Software, San Diego, CA). Unless the estimated K_s was within 5-fold of the P450 concentration, nonlinear regression analysis was applied using the hyperbolic equation: $\Delta A = B_{max}[L]/(K_s + [L])$, where A is the absorbance difference, B_{max} is the maximum absorbance difference extrapolated to infinite ligand concentration, and [L] is the ligand concentration [25].

2.9. Computational methods

The initial structure of wild-type CYP102A1 was obtained from the PDB database (http://www.rcsb.org) under the code 1BU7, and this was used as a starting structure. Only one half of the dimeric molecule, the monomer structure containing one complete binding site, was used for molecular docking and simulation. All water molecules and 1,2-ethanediols were removed from the X-ray structure of CYP102A1, and the hydrogen atoms were added by WHAT-IF software [26]. The structures of the mutants were also modeled *in silico* by the homology modeling program MODELLER [27]. The active site of CYP102A1 was examined by comparing it against the X-ray structure of palmitic acid-bound CYP102A1 (PDB code:

2UWH). The parameters embedded in the AMBER package suitable for use in energy minimization and molecular dynamics are available for different force fields [28,29]. The heme unit was simulated in its ferric resting state, corresponding to the X-ray structure. The force field parameters used for this study of a resting state heme in the P450s were developed by Harris et al. [30].

The geometries of all of the substrates (phenacetin and 7-ethoxyresorufin) were optimized using the Hartree–Fock method with a 6-31G* basis set, as implemented in the Gaussian 03 program [31]. The electrostatic potential charges were calculated, and the restrained electrostatic potential (RESP) procedure of the Antechamber program from the AMBER program suite was used to generate input files with charges for docking programs [32–35]. The generated result was used as a valid input for the AutoDock ligand preparation procedure.

Docking analysis was performed using AutoDock version 4.0, with the implemented empirical free energy function and the Lamarckian genetic algorithm [36]. Proportional selection was used, where the average of the worst energy was calculated over a window of ten generations. For the local search, the pseudo-Solis and Wets algorithms were applied using a maximum of 300 iterations per local search. One hundred independent docking runs were carried out for each substrate, and results differing by less than 1.0 Å in positional root mean-square deviation (RMSD) were clustered together and represented by the result with the most favorable free energy of binding. The best docked conformations were those found to have the lowest binding energy and the greatest number of members in the cluster, indicating good convergence. Both 1BU7 (wild-type) and its mutants were kept rigid during the docking process.

At the beginning of the molecular dynamics simulations for substrate-bound CYP102A1 complexes, all atoms were constrained with a finite force constant of 10 kcal/Å^2 for 10 ps. This constraint was then gradually reduced to 5, 1, 0.5, 0.1, and 0.05 kcal/Å^2 for a total of 90 ps. After the 100 ps of constrained molecular dynamics (MD), the constraint on all protein residues was removed. A 1 ns MD simulation was then performed, and the coordinates were recorded every 0.2 ps. During the entire period of the simulation, the temperature was kept at 300 K. A long, non-bonding cutoff of 15 Å was used to minimize large forces associated with truncations in the non-bonded interactions. Since explicit solvents were included in the system, a dielectric constant of unity was used. The best orientation was identified and optimized using the scoring function based on the AMBER force field FF99 and the energy minimization according to the Nelder and Mead algorithm [37] for induced-fit simulation. The orientations were then clustered and prioritized according to their score.

3. Results and discussion

3.1. Oxidation of human CYP1A2 substrates as catalyzed by CYP102A1 enzymes

The catalytic activities of CYP102A1 mutant enzymes toward three substrates that are known to be specifically oxidized by human CYP1A2 were investigated. First, the ability of wild-type CYP102A1 and a set of mutants to act upon human CYP1A2 substrates was measured at a fixed substrate concentration (7-methoxyresorufin, 2.0 μM; 7-ethoxyresorufin, 2.0 μM; and phenacetin, 2.0 mM) (Fig. 2).

CYP102A1 enzymes converted phenacetin into one major metabolite (Fig. 2A), which was identified as acetaminophen by HPLC analysis (Fig. 3) and LC–MS comparison with the authentic standard compound, acetaminophen. The catalytically active mutants of CYP102A1 produced only one major product, which had a retention time that exactly matched the acetaminophen standard. Oxidation products of phenacetin catalyzed by human CYP1A2 were the known acetaminophen and acetol products [18]. However, the metabolite acetol was not formed by CYP102A1 enzymes. The turnover numbers for the entire set of 17 mutants for *O*-deethylation of phenacetin varied over a 23-fold range. We found that wild-type CYP102A1 showed very low activity under the examined conditions (Fig. 2A) (0.47 min^{-1} for PhOD). The activity of CYP102A1 mutant #17 was approximately 11-fold higher than that of human CYP1A2.

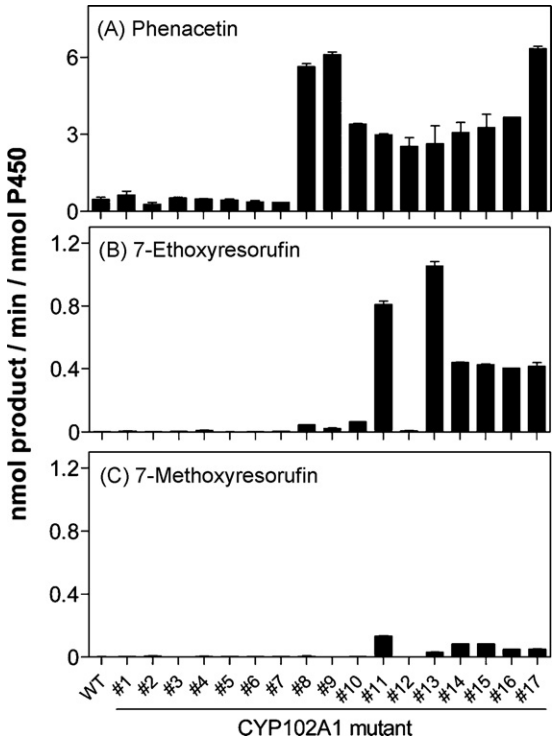

Fig. 2. *O*-Dealkylation reactions of human CYP1A2 substrates catalyzed by CYP102A1 mutants. Each substrate (2.0 mM phenacetin, 2.0 μM 7-ethoxyresorufin, and 2.0 μM 7-methoxyresorufin) was incubated with 50 pmol of each indicated CYP102A1 mutant in 100 mM potassium phosphate buffer (pH 7.4). *O*-Dealkylation reactions of phenacetin (A) and alkoxyresorufin (B and C) were quantified using HPLC and fluorescence analysis, respectively.

MROD and EROD activities of CYP102A1 mutants were also examined (Fig. 2B and C), and the metabolite was identified as resorufin by spectrofluorimetric analysis with the authentic standard compound, resorufin (results not shown). The alkoxyresorufin *O*-deethylation activities varied over a wide range. In general, MROD activities catalyzed by CYP102A1 mutants were much lower than those of EROD. Although mutant #11 showed the highest reaction rate (0.133 min^{-1}) for MROD among all mutants, its EROD activity was only 13% of mutant #13 (1.06 min^{-1}). Interestingly, mutants #8–10 and #12 did not show apparent activities toward 7-ethoxyresorufin and 7-methoxyresorufin but did show high activity (2.6 min^{-1}) toward PhOD. Notably, the *O*-deethylation activities of 7-methoxyresorufin and 7-ethoxyresorufin by CYP102A1 mutants #11 and #13 were 43- and 430-fold higher than that of CYP102A1 wild-type, respectively.

The kinetic parameters (k_{cat} and K_m) of catalysis by CYP102A1 mutants were compared using two typical human CYP1A2 substrates: 7-ethoxyresorufin and phenacetin (Tables 1 and 2). Each set of five mutants was chosen and used to measure kinetic parameters for EROD and PhOD, respectively (Tables 1 and 2). Mutants #13 and #12 were used for EROD and PhOD, respectively, although others were used for both assays. Some mutants of CYP102A1 did not

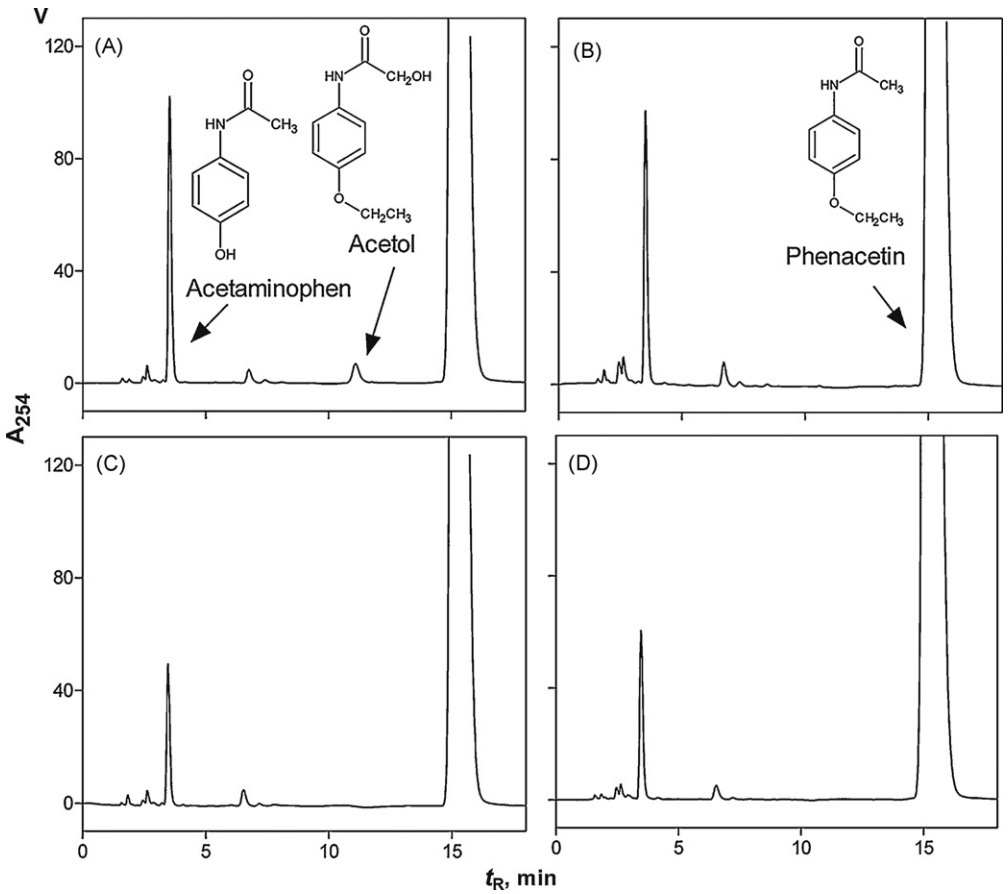

Fig. 3. HPLC trace of phenacetin metabolite produced by CYP102A1 enzymes. Phenacetin (2 mM) was incubated with 50 pmol CYP1A2 or CYP102A1 enzyme in 100 mM potassium phosphate buffer (pH 7.4): (A) CYP1A2, (B) mutant #8, (C) mutant #11, and (D) mutant #16.

show any appreciable activities with which to determine reliable kinetic parameters (Fig. 2). However, mutants #11, #13, #14, and #15 showed significantly elevated k_{cat} values for the EROD reaction, which were 2.0- to 2.8-fold higher than that of human CYP1A2. Mutants #14 and #15 had the highest k_{cat} values of 6.5 min^{-1}. The overall K_m values ranged from 3.0 to 6.3 μM, with values 8.1- to 17-fold higher than that of human CYP1A2. These mutants displayed 3.4- and 2.1-fold variations in k_{cat} and K_m values for the EROD reaction, respectively (Table 1), and their catalytic efficiencies (k_{cat}/K_m) varied 3.7-fold. Kinetic parameters of MROD by CYP102A1 mutants were not determined because the activities measured were too low for reliable calculations.

Table 1
Kinetic parameters of 7-ethoxyresorufin *O*-deethylation activity by CYP102A1 mutants.

P450	k_{cat} (min^{-1})	K_m (μM)	k_{cat}/K_m
Mutant #11	5.0 ± 0.1	5.0 ± 0.1	1.0 ± 0.1
#13	4.6 ± 0.1	3.0 ± 0.5	1.5 ± 0.3
#14	6.5 ± 0.1	6.3 ± 0.3	1.0 ± 0.1
#15	6.5 ± 0.2	6.2 ± 0.6	1.0 ± 0.1
#16	1.9 ± 0.1	4.6 ± 0.5	0.41 ± 0.05
Human CYP 1A2	2.3 ± 0.2	0.37 ± 0.10	6.2 ± 1.8

Table 2
Kinetic parameters of phenacetin *O*-deethylation activity by CYP102A1 mutants.

P450	k_{cat} (min^{-1})	K_m (μM)	k_{cat}/K_m
Mutant #11	8.2 ± 1.1	1480 ± 360	0.0055 ± 0.0015
#12	5.3 ± 0.8	2090 ± 530	0.0025 ± 0.0007
#14	4.6 ± 0.2	455 ± 66	0.010 ± 0.002
#15	5.8 ± 0.3	506 ± 78	0.011 ± 0.002
#16	8.5 ± 0.6	1370 ± 170	0.0062 ± 0.0009
Human CYP 1A2	2.0 ± 0.1	16 ± 3	0.13 ± 0.03

Several mutants showed significantly elevated k_{cat} values for the PhOD reaction (Table 2). Mutant #16 had the highest k_{cat} value of 8.5 min^{-1}, and the overall K_m values ranged from 455 to 2090 μM. The mutants displayed 1.8- and 4.6-fold variations in k_{cat} and K_m values for the PhOD reactions, respectively (Table 2). The k_{cat} values of the highest active mutant for EROD and PhOD by CYP102A1 enzymes were 2.8- and 4.3-fold, respectively, higher than those of human CYP1A2 enzyme. However, all K_m values of CYP102A1 mutants were significantly increased when compared to that of human CYP1A2. In general, the catalytic efficiencies (k_{cat}/K_m) for most of the reactions catalyzed by CYP102A1 enzymes were lower than those of CYP1A2 due to a significant increase in K_m values.

When the TTNs (mol product/mol catalyst) of the CYP102A1 mutants were determined using 7-ethoxyresorufin and phenacetin, the overall values ranged from 13 to 107 and from 455 to 932, respectively (Fig. 4). Mutants #8 and #11 showed the highest TTN values for PhOD and EROD activities, respectively. Resorufin, produced by human CYP1A2 and mutant #12, could not be detected after 6 h incubation. Mutant #8 showed high TTNs activity with phenacetin and 7-ethoxyresorufin. Although mutant #8 showed low catalytic activities for both substrates under the test conditions, it displayed high TTNs with phenacetin and 7-ethoxyresorufin. The catalytic activity of mutant #8 as shown was not saturated at the highest concentration (2.0 mM) of phenacetin. This result suggests the possibility that CYP102A1 mutants can be

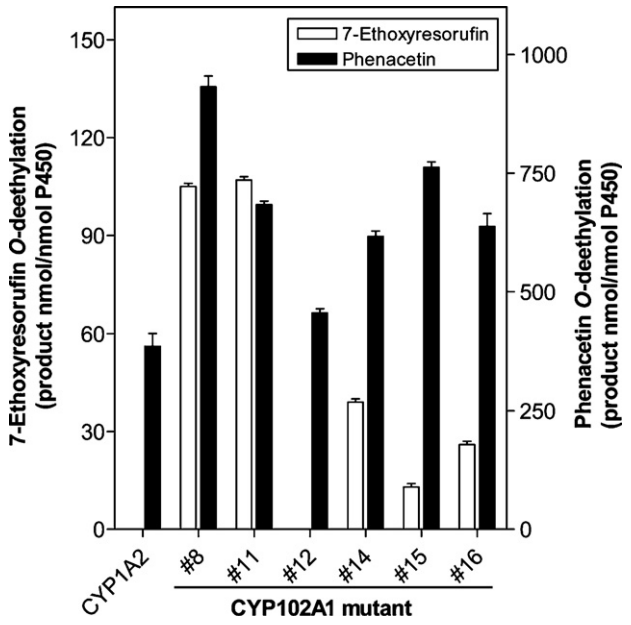

Fig. 4. Total turnover numbers (TTNs) of alkoxyresorufin and phenacetin *O*-deethylation activity by CYP102A1 mutants. Reaction mixtures consisted of 50 pmol P450, 100 mM potassium phosphate buffer (pH 7.4), an NADPH-generating system, and substrate (2.0 mM and 20 μM of phenacetin and 7-ethoxyresorufin, respectively). The reaction mixtures were incubated at 30 °C for 6 h. The products of phenacetin and 7-ethoxyresorufin were analyzed by HPLC and fluorometer, respectively.

developed as biocatalysts to produce drug metabolites, which are biologically generated by human CYP1A2.

3.2. Binding of human CYP1A2 substrates to the CYP102A1 enzymes

Ferric CYP102A1 enzymes exhibited a low-spin state, and the addition of substrate (phenacetin) produced a conversion in the spin-state depending on the different mutant types of CYP102A1 enzyme (Supplemental Fig. 1). Binding affinities of phenacetin to CYP102A1 mutants were estimated spectrophotometrically by monitoring the heme spectral changes upon the addition of ligands. K_s values were obtained from the titration curves, as described in Section 2.

The binding spectrum of CYP102A1 mutants resulted in a Type II shift in the heme Soret band upon binding to phenacetin, with a decrease in absorbance at 390 nm and an increase in absorbance at 420 nm. The binding affinities of CYP102A1 enzymes to phenacetin were determined: mutants #11 ($K_s = 1830 \pm 110$ μM) (Supplemental Fig. 1A); #14 ($K_s = 4140 \pm 290$ μM) (Supplemental Fig. 1B); #15 ($K_s = 1780 \pm 130$ μM) (Supplemental Fig. 1C); and #16 ($K_s = 1030 \pm 70$ μM) (Supplemental Fig. 1D). It was reported that phenacetin results in a Type II shift in the heme Soret band of human CYP1A2, with a decrease in absorbance at 390 nm and an increase in absorbance at 420 nm, typical of a ligand (nitrogen atom) coordinating the heme iron [38]. The binding affinity of human CYP1A2 ($K_s = 14 \pm 2$ μM) to phenacetin [24] was much higher than those of CYP102A1 mutants (Supplemental Fig. 1). At present, we cannot explain the reason why the K_s values of mutants #11, #14, and #15 are higher than the K_m values of those mutants. This result may indicate that multiple ligand binding sites exist inside the active site of the mutants.

Addition of 7-methoxyresorufin and 7-ethoxyresorufin to the CYP102A1 mutants (up to 2.0 mM) did not show any apparent change of the low-spin state of the heme.

3.3. Effects of human CYP1A2 inhibitor on the CYP102A1 enzymes

It is known that αNF binds tightly to human CYP1A2 to competitively inhibit its activity [16]. In this work, we examined the effect of αNF on the catalytic activities of CYP102A1 mutants that had human CYP1A2 activities. A single concentration (200 μM) of αNF was added to reactions containing phenacetin and 7-ethoxyresorufin (Fig. 5). The *O*-deethylation activities of phenacetin and 7-ethoxyresorufin by human CYP1A2 were inhibited by 88% and 93%, respectively, following addition of αNF. PhOD activities of CYP102A1 mutants #4, #5, and #13 were inhibited by ~90%, but those of the other CYP102A1 enzymes were only inhibited by approximately 40–60% by αNF. The EROD activities of CYP102A1 mutants #11, #13, #14, #15, #16, and #17 were inhibited by 45–65% (Fig. 5B). However, PhOD activity of CYP102A1 mutants #15 and #16 increased by 50–100% (Fig. 5A). Although αNF did not show inhibitory effects on the catalytic activities of all tested CYP102A1 mutants with human CYP1A2 activities, these results show that αNF can bind to the active site of CYP102A1 mutants to change their catalytic activities.

A triple CYP102A1 mutant (R47L/F87V/L188Q) has the ability to metabolize typical mammalian P450s substrates, such as amodiaquine, dextromethorphan, acetaminophen, testosterone, and 3,4-methylenedioxymethylamphetamine [39]. Although the product formation of these chemicals by a triple CYP102A1 mutant were inhibited from 30% to 60% by αNF, the inhibitor did not have a significant effect on the metabolism of acetaminophen and 3,4-methylenedioxymethylamphetamine.

3.4. Modeling of CYP102A1 mutants with substrates

Induced fit docking was performed to gain insight into the conformational changes that may occur in the binding site structure upon interaction with the reported substrates, with an aim of investigating the mechanism behind the hydroxylation reaction. Representative binding mode structures for phenacetin and 7-ethoxyresorufin in wild-type CYP102A1 and its mutant #15 (R47L/E64G/F87V/E143G/L188Q/E267V), as well as the conforma-

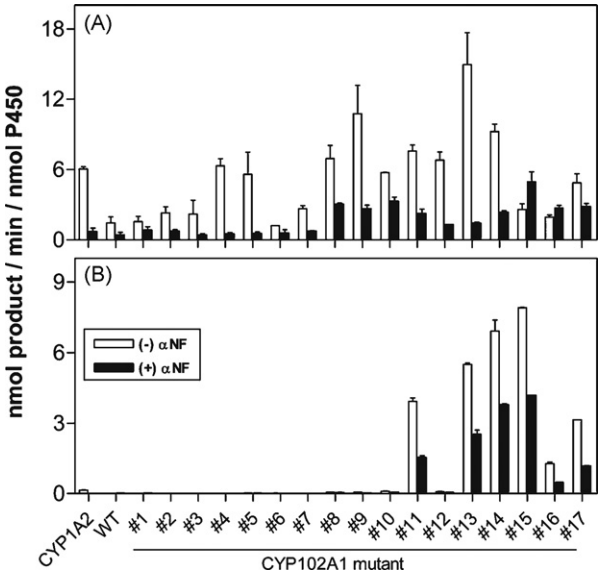

Fig. 5. Effect of αNF on *O*-dealkylation of human CYP1A2 substrates, phenacetin (A) and 7-ethoxyresorufin (B), catalyzed by wild-type CYP102A1 and mutant CYP102A1. Concentrations of phenacetin and 7-ethoxyresorufin were set at 2 mM and 20 μM, respectively. The catalytic activities were measured in the presence (closed square) and absence (open square) of 200 μM αNF. The effects of αNF on phenacetin *O*-dealkylation and EROD by human CYP1A2 are also shown.

tional changes induced in CYP102A1 structures as predicted by our induced fit docking simulations, are shown in Supplemental Fig. 2.

In wild-type CYP102A1, two compounds are predicted to bind with the ethoxyl substituent oriented toward the surface of the heme in its ferric resting state. Aromatic–aromatic contact (π–π) interactions between the aromatic ring substituent and residue F87 are likely to occur. At the other end of the two substrates, the hydrophilic substituent (the amide or the carbonyl group) of the aromatic ring is oriented to occupy the opposite part of the heme molecule in the binding pocket. While 7-ethoxyresorufin forms mainly hydrophobic interactions with the binding site residues in this region, the ethanamide group of phenacetin is capable of forming polar contacts because they are positioned within hydrogen bonding distance of M185. In mutant #15, the binding mode for 7-ethoxyresorufin is inclined to about 60° in comparison to the binding complex with the wide-type enzyme, whereas phenacetin binding to this mutant shifted toward the heme along the longest axis compared to the wild-type structure. Phenacetin and 7-ethoxyresorufin appear to lose all hydrophobic contact interactions in their alternate binding mode in mutant #15 (Fig. 6 and Supplemental Table 1).

On closer inspection, distinguishable binding conformations of phenacetin were observed within complexes with wide-type CYP102A1 and mutant #15, in which positioning of the phenacetin is subtly but significantly altered from the wide-type to mutant #15 structure. In the wide-type CYP102A1 complex with phenacetin (Fig. 6A), an almost planar π–π stacking interaction between F87 and the phenyl ring of phenacetin is formed. In the mutant #15 complex, however, this interaction is lost, but instead further interaction occurs between the carbon (C^{EtO}) connected to an ethoxyl phenyl oxygen of phenacetin and the iron atom in the heme (Fig. 6C) in comparison with the wide-type CYP102A1 complex. The wide-type CYP102A1 complex has a Fe/C^{EtO} distance of 4.27 Å (Fig. 6A), and the corresponding mutant #15 complex has a Fe/C^{EtO} distance of 3.12 Å (Fig. 6C).

The central phenoxazin ring at the base of 7-ethoxyresorufin can potentially form non-polar interactions in both subset complexes of wide-type CYP102A1 and mutant #15 with similar residues, except for residue 87: in the wide-type CYP102A1 complex, phenoxazin interacts primarily with V78, F87, M185, and L437 (Fig. 6B); whereas in the mutant #15 complex, it is much further from L437 and instead proximal to V87 (Fig. 6D). It emerges that the carbon connected to an ethoxy group of 7-ethoxyresorufin is located in closer proximity to the iron of the heme in the mutant #15 complex (distance of 3.25 Å, Fig. 6D) than in the wide-type CYP102A1 complex (distance of 4.39 Å, Fig. 6B).

The docking simulations suggest that binding of phenacetin and 7-ethoxyresorufin to mutant #15 entails reorientation of only a few residues (M185, I263, A328, P329, A330, and M354 in particular) compared to their orientations in the initial crystal structure used as the starting model for the induced fit dockings. In the wide-type, a similar rearrangement is only observed when fitting phenacetin and 7-ethoxyresorufin into the binding pocket (Supplemental Fig. 3). On the basis of the induced fit docking results, one can hypothesize that the *O*-deethylation reaction observed for the two substrates arises structurally from movement of several residues, shown in Supplemental Table 1, since no other major modifications are predicted to take place according to these representative binding modes. The movement of these residues may, in turn, lead to the more extensive structural changes required for the *O*-deethylation reaction. Superimposition of the structures of CYP102A1 and mutant #15 show that the β-sheet structures, constituting the entry site for the substrate, is induced into a different

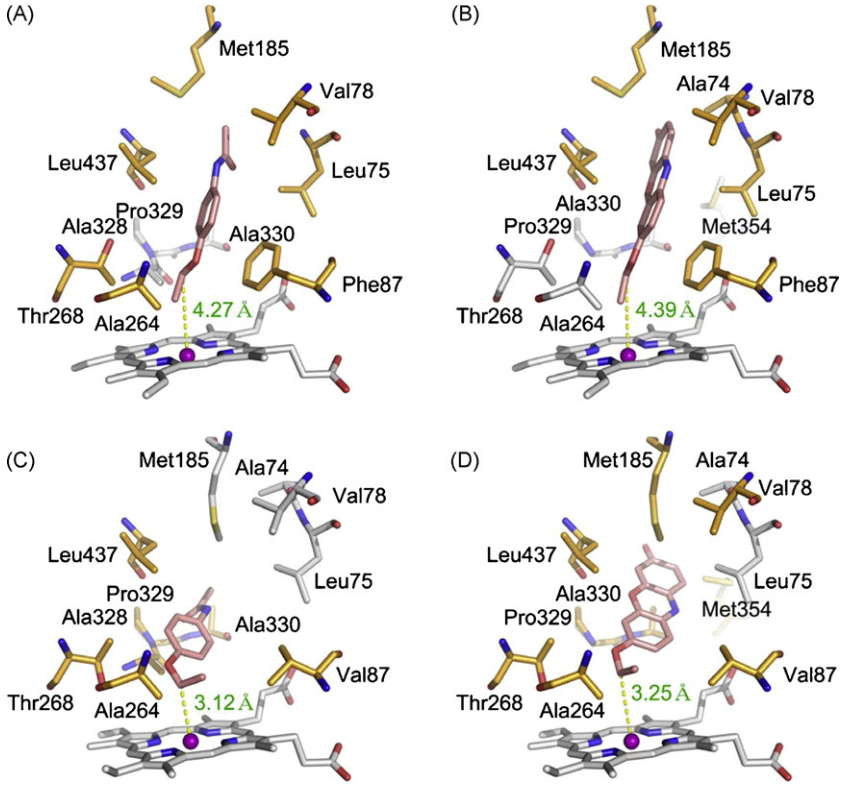

Fig. 6. Interaction modes of phenacetin (A and C) and 7-ethoxyresorufin (B and D) in the active sites of wild-type CYP102A1 (A and B) and mutant #15 (C and D) in the close vicinity of two substrates (<4 Å). The residues involved in the binding interaction with substrate are color-coded as light orange. The distance between the carbon (C^{EtO}) connected to an ethoxyl phenyl oxygen of phenacetin (A and C) or 7-ethoxyresorufin (B and D) and the iron atom in the heme is shown. (For interpretation of the references to color in this figure legend, the reader is referred to the web version of the article.)

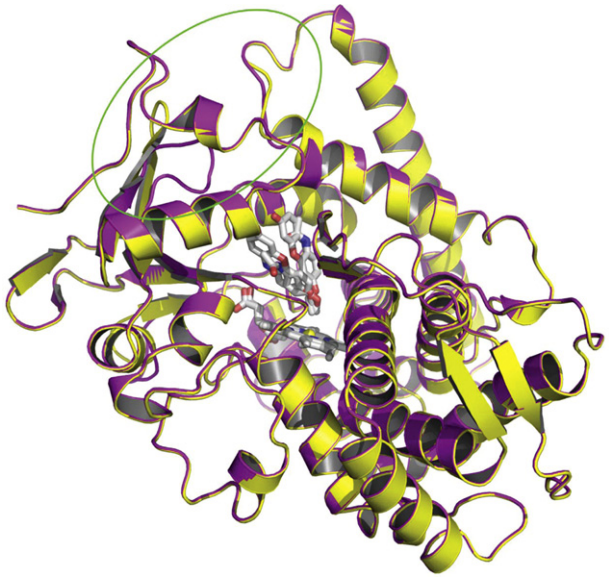

Fig. 7. Superimposition of the structures of CYP102A1 (yellow) and mutant #15 (violet) complexes with their substrates (phenacetin and 7-ethoxyresorufin). The superimposition shows that the β-sheet structures constituting the entry site for the substrate change conformation in the mutant (circle). (For interpretation of the references to color in this figure legend, the reader is referred to the web version of the article.)

conformation by the amino acid substitutions (Fig. 7). Further, side chain movements are required to optimally fit phenacetin and 7-ethoxyresorufin into the active sites of CYP102A1 and mutant #15. These side chain adjustments resulting from the decreased cavity size may mechanistically be related to the origin of the cavity size of active sites.

4. Conclusion

This study examined the interaction of a set of CYP102A1 mutants and some typical substrates of human CYP1A2 and revealed that bacterial CYP102A1 enzymes catalyze the same reactions as human CYP1A2. The oxidations of phenacetin, 7-methoxyresorufin, and 7-ethoxyresorufin (typical substrates of human CYP1A2) were catalyzed by some mutants of CYP102A1. In the case of PhOD reactions, one major product, acetaminophen, was produced as a result of the human CYP1A2 reaction. The other biological hydroxylated product, acetol, was not produced with the bacterial enzyme. Acetaminophen formation was confirmed by HPLC analysis and LC–MS, comparing the metabolite with the authentic acetaminophen compound. Catalytic activities of some CYP102A1 mutants were higher than those of human CYP1A2. Also, some mutants of CYP102A1 were not inhibited by αNF, a known competitive inhibitor of human CYP1A2. The similar oxidation profiles and highly catalytic activities of CYP102A1 mutants on human CYP1A2 substrates suggest that these bacterial enzymes may represent a model system for studying the human enzymes. The computational findings further imply that a conformational change in the active site cavity size is related to the change in activity in the CYP102A1 mutants. It can be proposed that the activity change results from movement of several residues in the active site.

Acknowledgments

This work was supported in part by the 21C Frontier Microbial Genomics and the Application Center Program of the Ministry of Education, Science and Technology of the Republic of Korea; the Korea Science and Engineering Foundation [Grant R01-2008-000-21072-02008]; and the Second Stage BK21 Project from the Ministry of Education, Science and Technology of the Republic of Korea.

Appendix A. Supplementary data

Supplementary data associated with this article can be found, in the online version, at doi:10.1016/j.molcatb.2010.01.017.

References

[1] F.P. Guengerich, Chem. Res. Toxicol. 22 (2009) 237–238.
[2] V.B. Urlacher, S. Eiben, Trends Biotechnol. 24 (2006) 324–330.
[3] C.H. Yun, K.H. Kim, D.H. Kim, H.C. Jung, J.G. Pan, Trends Biotechnol. 25 (2007) 289–298.
[4] B.M. van Vugt-Lussenburg, E. Stjernschantz, J. Lastdrager, C. Oostenbrink, N.P. Vermeulen, J.N. Commandeur, J. Med. Chem. 50 (2007) 455–461.
[5] M.D. Johnson, H. Zuo, K.H. Lee, J.P. Trebley, J.M. Rae, R.V. Weatherman, Z. Desta, D.A. Flockhart, T.C. Skaar, Breast Cancer Res. Treat. 85 (2004) 151–159.
[6] C.R. Otey, G. Bandara, J. Lalonde, K. Takahashi, F.H. Arnold, Biotechnol. Bioeng. 93 (2006) 494–499.
[7] D.H. Kim, K.H. Kim, K.H. Liu, H.C. Jung, J.G. Pan, C.H. Yun, Drug Metab. Dispos. 36 (2008) 2166–2170.
[8] D.H. Kim, T. Ahn, H.C. Jung, J.G. Pan, C.H. Yun, Drug Metab. Dispos. 37 (2009) 932–936.
[9] M. Landwehr, L. Hochrein, C.R. Otey, A. Kasrayan, J.E. Backvall, F.H. Arnold, J. Am. Chem. Soc. 128 (2006) 6058–6059.
[10] A.M. Sawayama, M.M. Chen, P. Kulanthaivel, M.S. Kuo, H. Hemmerle, F.H. Arnold, Chemistry 15 (2009) 11723–11729.
[11] M.C. Damsten, J.S. de Vlieger, W.M. Niessen, H. Irth, N.P. Vermeulen, J.N. Commandeur, Chem. Res. Toxicol. 21 (2008) 2181–2187.
[12] M.C. Damsten, B.M. van Vugt-Lussenburg, T. Zeldenthuis, J.S. de Vlieger, J.N. Commandeur, N.P. Vermeulen, Chem. Biol. Interact. 171 (2008) 96–107.
[13] E. Stjernschantz, B.M. van Vugt-Lussenburg, A. Bonifacio, S.B. de Beer, G. van der Zwan, C. Gooijer, J.N. Commandeur, N.P. Vermeulen, C. Oostenbrink, Proteins 71 (2008) 336–352.
[14] B.M. Lussenburg, L.C. Babel, N.P. Vermeulen, J.N. Commandeur, Anal. Biochem. 341 (2005) 148–155.
[15] F.P. Guengerich, T. Shimada, Mutat. Res. 400 (1998) 201–213.
[16] S. Sansen, J.K. Yano, R.L. Reynald, G.A. Schoch, K.J. Griffin, C.D. Stout, E.F. Johnson, J. Biol. Chem. 282 (2007) 14348–14355.
[17] D.J. Waxman, T.K. Chang, Methods Mol. Biol. 320 (2006) 153–156.
[18] C.H. Yun, G.P. Miller, F.P. Guengerich, Biochemistry 39 (2000) 11319–11329.
[19] A.B. Carmichael, L.L. Wong, Eur. J. Biochem. 268 (2001) 3117–3125.
[20] Q.S. Li, J. Ogawa, R.D. Schmid, S. Shimizu, Appl. Environ. Microbiol. 67 (2001) 5735–5739.
[21] T. Omura, R. Sato, J. Biol. Chem. 239 (1964) 2379–2385.
[22] M.D. Burke, R.T. Mayer, Chem. Biol. Interact. 45 (1983) 243–258.
[23] J. Liu, S.S. Ericksen, M. Sivaneri, D. Besspiata, C.W. Fisher, G.D. Szklarz, Arch. Biochem. Biophys. 424 (2004) 33–43.
[24] D.H. Kim, K.H. Kim, E.M. Isin, F.P. Guengerich, H.Z. Chae, T. Ahn, C.H. Yun, Protein Expr. Purif. 57 (2008) 188–200.
[25] E.M. Isin, F.P. Guengerich, J. Biol. Chem. 281 (2006) 9127–9136.
[26] G. Vriend, J. Mol. Graph. 8 (1990) 52–56, 29.
[27] A. Sali, T.L. Blundell, J. Mol. Biol. 234 (1993) 779–815.
[28] Y. Duan, C. Wu, S. Chowdhury, M.C. Lee, G. Xiong, W. Zhang, R. Yang, P. Cieplak, R. Luo, T. Lee, J. Caldwell, J. Wang, P. Kollman, J. Comput. Chem. 24 (2003) 1999–2012.
[29] J. Wang, R.M. Wolf, J.W. Caldwell, P.A. Kollman, D.A. Case, J. Comput. Chem. 25 (2004) 1157–1174.
[30] D.L. Harris, J.Y. Park, L. Gruenke, L. Waskell, Proteins 55 (2004) 895–914.
[31] M.J. Frisch, G.W. Trucks, H.B. Schlegel, G.E. Scuseria, M.A. Robb, J.R. Cheeseman, J.A. Montgomery, Jr., T. Vreven, K.N. Kudin, J.C. Burant, J.M. Millam, S.S. Iyengar, J. Tomasi, V. Barone, B. Mennucci, M. Cossi, G. Scalmani, N. Rega, G.A. Petersson, H. Nakatsuji, M. Hada, M. Ehara, K. Toyota, R. Fukuda, J. Hasegawa, M. Ishida, T. Nakajima, Y. Honda, O. Kitao, H. Nakai, M. Klene, X. Li, J.E. Knox, H.P. Hratchian, J.B. Cross, V. Bakken, C. Adamo, J. Jaramillo, R. Gomperts, R.E. Stratmann, O. Yazyev, A.J. Austin, R. Cammi, C. Pomelli, J.W. Ochterski, P.Y. Ayala, K. Morokuma, G.A. Voth, P. Salvador, J.J. Dannenberg, V.G. Zakrzewski, S. Dapprich, A.D. Daniels, M.C. Strain, O. Farkas, D.K. Malick, A.D. Rabuck, K. Raghavachari, J.B. Foresman, J.V. Ortiz, Q. Cui, A.G. Baboul, S. Clifford, J. Cioslowski, B.B. Stefanov, G. Liu, A. Liashenko, P. Piskorz, I. Komaromi, R.L. Martin, D.J. Fox, T. Keith, M.A. Al-Laham, C.Y. Peng, A. Nanayakkara, M. Challacombe, P.M.W. Gill, B. Johnson, W. Chen, M.W. Wong, C. Gonzalez, J.A. Pople, Gaussian 03, revision C.02, Inc., Wallingford, CT, 2004.
[32] P. Rydberg, L. Olsen, P.O. Norrby, U. Ryde, J. Chem. Theory Comput. 3 (2007) 1765–1773.
[33] L. Tian, R.A. Friesner, J. Chem. Theory Comput. 5 (2009) 1421–1431.
[34] D.A. Pearlman, D.A. Case, J.W. Caldwell, W.S. Ross, T.E. Cheatham, S. Debolt, D. Ferguson, G. Seibel, P. Kollman, Comput. Phys. Commun. 91 (1995) 1–41.

[35] D.A. Case, T.E. Cheatham, T. Darden, H. Gohlke, R. Luo, K.M. Merz, A. Onufriev, C. Simmerling, B. Wang, R.J. Woods, J. Comput. Chem. 26 (2005) 1668–1688.
[36] R. Huey, G.M. Morris, A.J. Olson, D.S. Goodsell, J. Comput. Chem. 28 (2007) 1145–1152.
[37] J.A. Nelder, R. Mead, Comput. J. 7 (1965) 308–313.
[38] J.B. Schenkman, H. Remmer, R.W. Estabrook, Mol. Pharmacol. 3 (1967) 113–123.
[39] B.M. van Vugt-Lussenburg, M.C. Damsten, D.M. Maasdijk, N.P. Vermeulen, J.N. Commandeur, Biochem. Biophys. Res. Commun. 346 (2006) 810–818.